Nuclear structure of ^{24}Mg: ^{23}Na(^{3}He, d) reaction

J. D. Garrett,* H. T. Fortune,† R. Middleton, and W. Scholz‡
Department of Physics, University of Pennsylvania, Philadelphia, Pennsylvania 19104
(Received 27 February 1978)

The states of ^{24}Mg below 11 MeV have been studied using the ^{23}Na(^{3}He,d) reaction at a bombarding energy of 15 MeV. Angular distributions of the reaction products have been compared with distorted-wave Born-approximation predictions. The resulting spectroscopic factors are compared with those calculated using the Nilsson model and with experimental spectroscopic factors of previous ^{23}Na(^{3}He,d) and ^{23}Na(d,n) studies. Several new rotational bands based on collective-model configurations are suggested. The experimentally measured spectroscopic factors for states based on the $(3/2^+[211])^2$, the $3/2^+[211]$, $1/2^+[211]$, and the $3/2^+[211]$, $1/2^-[330]$ Nilsson configurations are in general agreement with the predictions of the simple Nilsson model assuming large deformations. It is necessary to assume that the $T = 1$ states are less deformed than the $T = 0$ states in order to explain the properties of the low-lying $T = 1$ states in terms of the collective model.

[NUCLEAR REACTIONS ^{23}Na(^{3}He,d), E=15.0 MeV; measured $\sigma(E_d, \theta)$. ^{24}Mg deduced levels, J, π, S. DWBA analysis. Comparison with Nilsson model.]

I. INTRODUCTION

The low-lying levels of ^{24}Mg have been explained[1] in terms of the collective model[2] as members of $K^\pi = 0^+$ and 2^+ rotational bands. In this model, the $K^\pi = 0^+$ ground-state band is described as having the $\Omega^\pi[Nn_z\Lambda] = \frac{1}{2}^+[220]$ and $\frac{3}{2}^+[211]$ Nilsson orbitals completely filled. The $K^\pi = 2^+$ band has been assigned[3] as arising from unpaired nucleons in the $\frac{3}{2}^+[211]$ and $\frac{1}{2}^+[211]$ Nilsson orbitals coupled to $K = 2$. The excitation energies of the known[1,4-6] members of the two bands are shown in Fig. 1, along with the predicted[7] excitation energies obtained from SU(3) calculations. Measurements[8] of the intrinsic quadrupole moment of the first excited state of ^{24}Mg ($Q_0 = 0.661 \pm 0.020$b) are consistent with a deformation $\delta = 0.58$, which also accounts for the moments of inertia of the observed rotational bands.

Experimentally, the energy levels of ^{24}Mg up to 12 MeV were established by the ^{23}Na(^{3}He, d)^{24}Mg reaction[9] and by the ^{12}C(^{16}O, α)^{24}Mg reaction.[10] The spins, parities, isospins, and γ-ray branching ratios of the low-lying levels of ^{24}Mg are summarized in Refs. 4, 11, and 12. Spins, parities, and widths have been measured for higher-lying levels from resonances in the ^{23}Na(p,γ) reaction,[13] the ^{23}Na(p,p) reaction,[14] the ^{20}Ne(α,α) reaction,[15] and the ^{20}Ne(α,γ) reaction.[16] Single-nucleon spectroscopic information is available from studies of the ^{23}Na(d,n) reaction,[12,17] the ^{23}Na(^{3}He, d) reaction,[3] the ^{25}Mg(p, d) reaction,[18,19] the ^{25}Mg(d,t) reaction,[20] and the ^{25}Mg(^{3}He, α) reaction.[21] The two-nucleon transfer reactions have also yielded[22] information for some of the low-lying levels of ^{24}Mg.

Recently, several high angular momentum states[23-25] have been observed between excitations of 16 and 17 MeV in ^{24}Mg. These states were selectively populated in the ^{16}O(^{12}C, α) and ^{12}C(^{16}O, α) reactions.[23,25] The two known rotational bands (Fig. 1) cannot account for all the high-spin states that were observed. Strong ^{20}Ne(^{7}Li, t)^{24}Mg and ^{20}Ne(^{6}Li, d)^{24}Mg transitions[26-28] have also been observed. Additional information on the structure of the ^{24}Mg states in

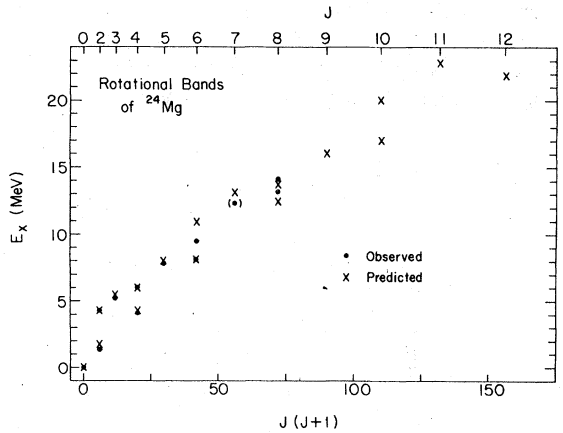

FIG. 1. Plot of excitation energies versus $J(J+1)$ for the members of the ground state and lowest $K^\pi = 2^+$ rotational bands in ^{24}Mg. The excitation energies of the assigned members (Refs. 4–6, 11, 24) are denoted by dots with a tentative assignment of the 7^+ member of the $K^\pi = 2^+$ band (Ref. 6) shown as a dot in parentheses. The X's denote predicted excitations obtained from SU(3) calculations (Ref. 7).

the 7- to 10-MeV excitation range should assist in the interpretation of the heavy-ion and α-transfer results.

In the present work the study of the ^{23}Na(^{3}He, d) reaction has been extended to an excitation energy of 11 MeV. The previous ^{23}Na(^{3}He, d) reaction study[3] included only the seven lowest states of ^{24}Mg.

II. EXPERIMENTAL PROCEDURE

The ^{23}Na(^{3}He, d)^{24}Mg reaction was studied at an incident energy of 15 MeV using the ^{3}He beam from the University of Pennsylvania tandem Van de Graaff accelerator. Reaction products were momentum analyzed in $7\frac{1}{2}°$ intervals, starting at $3\frac{3}{4}°$ (lab), using a multiangle spectrograph. Deuterons were detected photographically in 50-μm Kodak NTB nuclear emulsions. Mylar foil (10 mils in thickness) was placed in front of the emulsions to absorb the elastically scattered ^{3}He and the α particles from the ^{23}Na(^{3}He, α) reaction. The target was 35 μg/cm^2 of NaI on a 20 μg/cm^2 natural C backing.

A deuteron spectrum measured at a laboratory angle of $11\frac{1}{4}°$ is shown in Fig. 2. Levels in ^{24}Mg are labeled with their excitation energy. Reaction products resulting from the carbon backing are identified by the symbol and the level number of the corresponding residual nucleus. Since the magnetic field used (13.86 kG) was outside the range of the spectrograph calibration,[29] accurate excitation energies were not obtained. The excitation energies referred to herein are those from Refs. 9 and 10.

Angular distributions of 30 deuteron groups leading to states of ^{24}Mg below 11 MeV are shown in Figs. 3–6. The error bars on the data points represent statistical errors and, in some cases, uncertainties in the separation of impurity groups from groups corresponding to the levels of ^{24}Mg. An error of 30%, due principally to uncertainty in target thickness, is assigned to the absolute cross-section scale.

III. ANALYSIS

The analysis of the angular distributions was performed using the distorted-wave Born-approximation (DWBA) code **DWUCK**.[30] For a single-nucleon stripping reaction the experimental cross section $\sigma_{\text{exp}}(\Theta)$ is related to the theoretical single-particle cross section $\sigma_{nlj}(\Theta)$ (calculated using code **DWUCK**) by the expression[30]

$$\sigma_{\text{exp}}(\Theta) = NC^2 \frac{2J_f+1}{2J_i+1} \sum_{nlj} S_{nlj} \frac{\sigma_{nlj}(\Theta)}{2j+1} , \tag{1}$$

where

$$C = \langle T_i T_{z_i} t t_z | T_f T_{z_f} \rangle . \tag{2}$$

Here J, T, and T_z are the spin, isospin, and z component of isospin, respectively; i and f refer to the target and residual nucleus, and n, l, j, t, and t_z are the quantum numbers of the transferred particle. The normalization factor N includes the overlap of the incident- and exciting-particle wave functions, and the spectroscopic factor S_{nlj} is a measure of the overlap of the target plus transferred particle with the final state of the residual nucleus.

The appropriate elastic scattering measurements were not available to determine the entrance- and exit-channel optical-model parameters. For light, deformed nuclei (where a simple optical-model

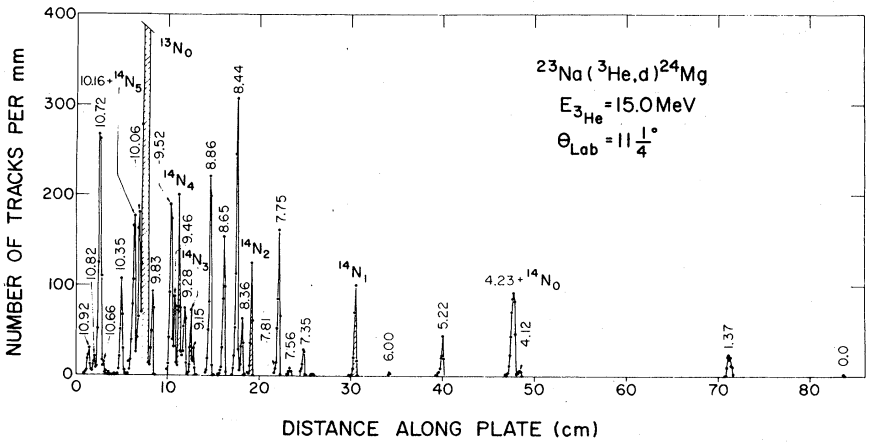

FIG. 2. Deuteron spectrum for the reaction ^{23}Na(^{3}He,d)^{24}Mg obtained at an incident energy of 15 MeV and a laboratory angle of 11.25°. Groups corresponding to reaction products from the carbon backing are hatched and are labeled by the excited states of the corresponding final nucleus.

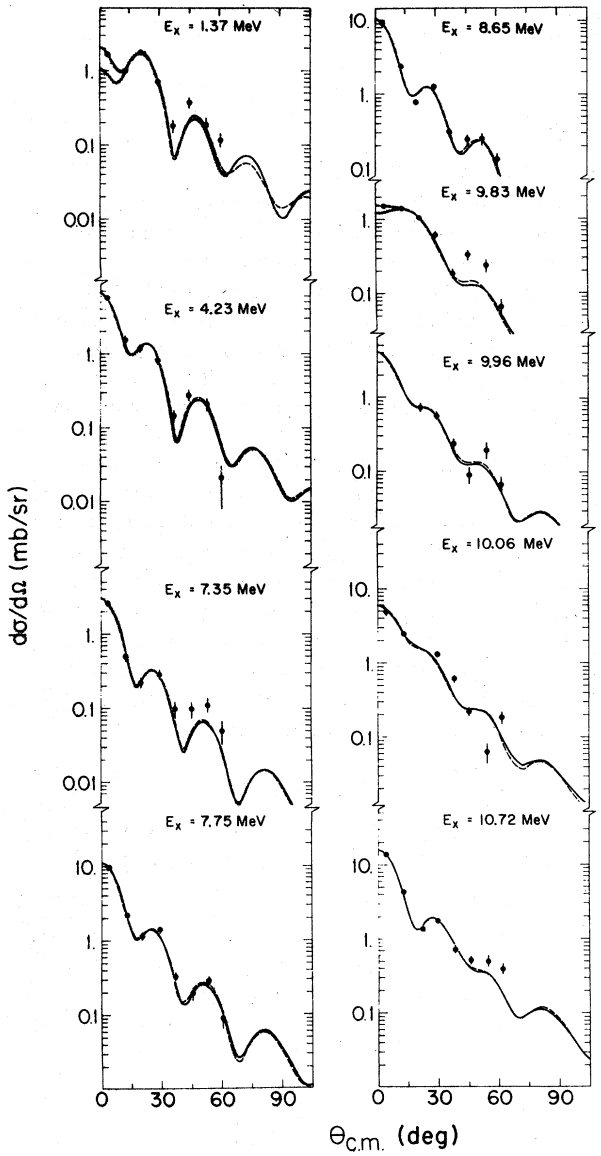

FIG. 3. Angular distributions which are characteristic of mixed $l=0$ and 2 ^{23}Na(^{3}He,d) transitions. The relative admixtures of $l=0$ and 2 were determined by a χ^2-minimization fit of the DWBA predictions to the experimental data. The solid and dashed curves correspond to $1d_{5/2}$ and $1d_{3/2}$ $l=2$ components, respectively. Pure $l=2$ ($1d_{5/2}$) DWBA predictions are shown as dotted curves for the 1.37- and 9.83-MeV levels.

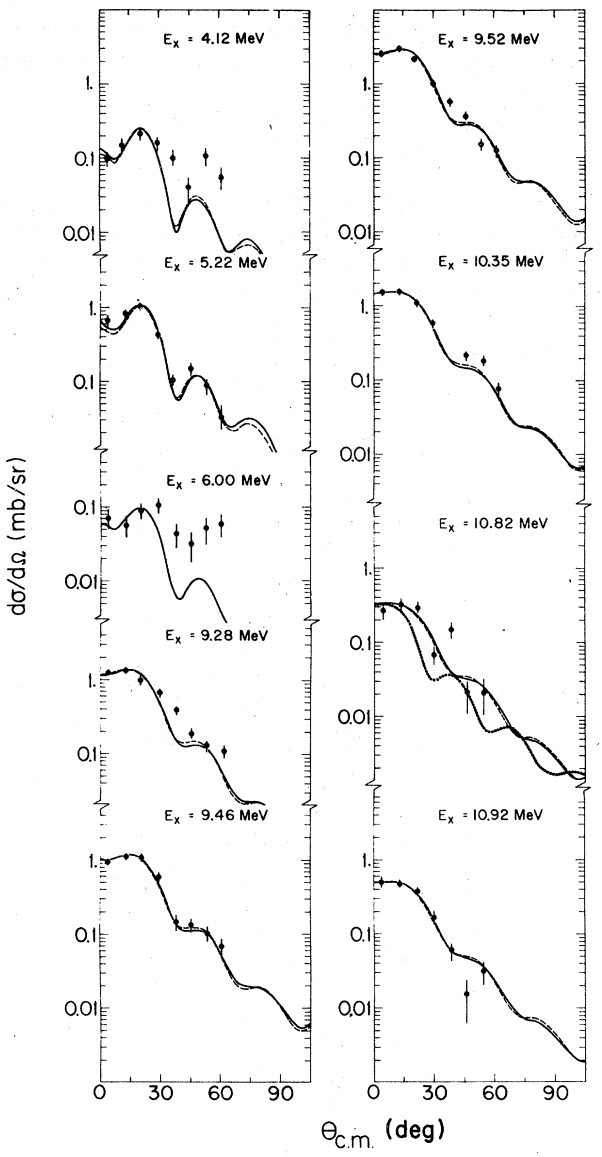

FIG. 4. Angular distributions exhibiting pure $l=2$ character in the ^{23}Na(^{3}He,d) reaction. The solid DWBA curves correspond to transfer to the $1d_{5/2}$ subshell and the dashed curve to the $1d_{3/2}$ subshell. A prediction based on an $l=1$ transition (dotted curve) is shown for comparison with the 10.82-MeV state.

description of the elastic scattering is probably not valid) better results are usually obtained in DWBA calculations by using average optical-model parameters applicable to the given energy and mass region. The optical-model parameters[31-35] used in the present analysis (listed in Table I) were the same as those used in recent (^{3}He, d) studies[31,32] on ^{21}Ne and ^{22}Ne. The calculations were all performed in the zero-range approximation using local potentials and a zero lower radial-integral cutoff. A conventional Thomas spin-orbit strength of $\lambda=25$ was used in the bound-state calculations even though it is known[36] that this value may lead to a reduced theoretical cross section (and hence to an increased spectroscopic factor, S_{nlj}) for $J=l-\frac{1}{2}$. The DWBA predictions are displayed along with the experimental data in Figs. 3 to 5.

The extracted spectroscopic factors [as defined in Eq. (1)] are compared below with those calculated from the Nilsson model, using the expression[37]

$$C^2S_{nlj} = g^2 \frac{2J_i+1}{2J_f+1} |\langle f|i\rangle|^2 |\langle j(K_f \mp K_i) J_i \pm K_i | J_f K_f\rangle|^2 |\langle \chi_f | a^\dagger | \chi_i\rangle|^2 , \quad (3)$$

where the various parameters are as defined above and in Ref. 31. The ground-state wave function of ^{23}Na, $|\chi_i\rangle$, was assumed to consist of paired neutrons and an unpaired proton in the $\frac{3}{2}^+[211]$ Nilsson orbit outside a closed ^{20}Ne core. Values of the matrix elements of Eq. (3) for various final state configurations populated in the ^{23}Na(^{3}He, d)^{24}Mg reaction are given in Table II. From the orthonormality of the Clebsch-Gordan coefficients, one obtains the in-band sum rules given in column five of Table II. The sum is over n, l, and j for all final states in a given rotational band.

The Nilsson expansion coefficients $W(\alpha, \nu)$ ($\alpha = N, n_z, \Lambda$, the Nilsson asymptotic quantum numbers[2] and $\nu = nljmt_z$, the shell-model quantum numbers of the transferred nucleon) that were used in the calculation of spectroscopic factors were calculated[31,38] for a proton in a deformed Woods-Saxon well. These coefficients are tabulated in Ref. 31. The binding energies of the deformed Woods-Saxon potential[31,38] are compared with the harmonic-oscillator results[39] in Fig. 7.

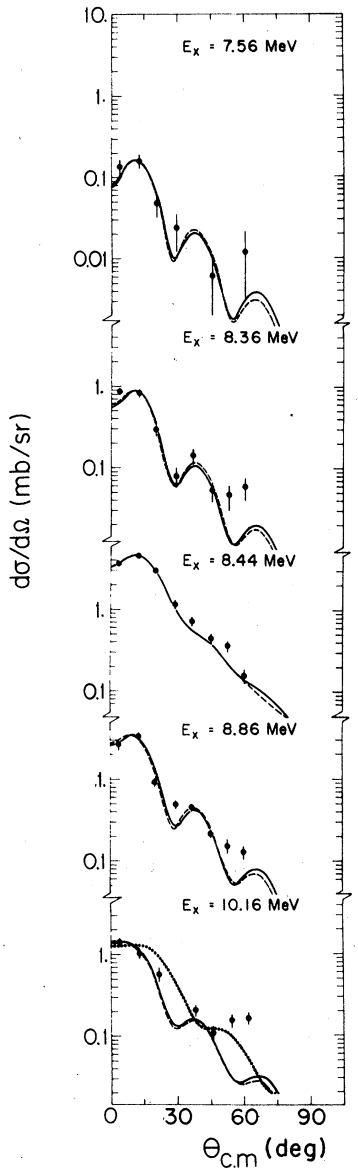

FIG. 5. Angular distributions exhibiting pure $l=1$ character in the ^{23}Na(^{3}He,d) reaction. The solid DWBA curves correspond to transfer to the $2p_{3/2}$ subshell and the dashed curves to the $2p_{1/2}$ subshell. A prediction based on an $l=2$ transition (dotted curve) is shown for comparison with the 10.16-MeV state.

IV. RESULTS

The ^{23}Na(^{3}He, d)^{24}Mg angular distributions have been divided into four categories: (1) mixed l

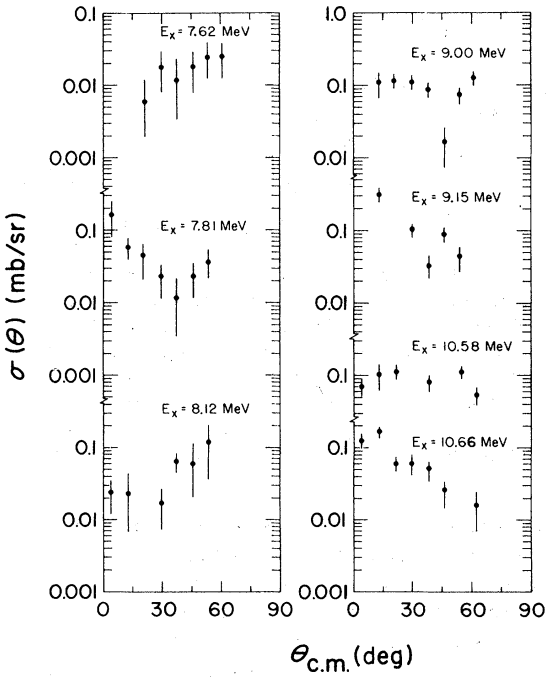

FIG. 6. Angular distributions for states excited weakly by the ^{23}Na(^{3}He,d)^{24}Mg reaction that are not characteristic of direct nucleon transfer.

TABLE I. Optical-model parameters used in the DWBA calculations.

Channel	V_0 (MeV)	W (MeV)	$W'=4W_D$ (MeV)	$r_0=r_{so}$ (F)	$a=a_{so}$ (F)	r_c (F)	r_0' (F)	a' (F)	V_{so} (MeV)	Reference
^{23}Na + ^{3}He	177.0	13.0	•••	1.138	0.7236	1.40	1.602	0.769	8.0	31–33
^{24}Mg + d	105.0	•••	80.0	1.02	0.86	1.30	1.42	0.65	6.0	31–34
Bound state	a	•••	•••	1.26	0.60	1.26	•••	•••	$\lambda=25$	35

[a] The bound-state well depths were adjusted to give the nucleons a binding energy of $B = [5.494 + Q(^3\mathrm{He}, d)]$ MeV.

$=0+2$ transitions (Fig. 3), (2) $l=2$ transitions (Fig. 4), (3) $l=1$ transitions (Fig. 5), and (4) weak transitions whose angular distributions show little structure (Fig. 6).

The angular distributions shown in Fig. 3 are characteristic of mixed $l=0+2$ (^{3}He, d) transitions. The relative admixtures of $l=0$ and 2 were determined by means of a χ^2-minimization fit to the experimental data. The $l=2$ contribution was calculated for both $1d_{5/2}$ transfer (solid lines) and $1d_{3/2}$ transfer (broken lines). The peak DWBA cross section for $l=0$ single-particle transfer is an order of magnitude greater than the peak cross section for $l=2$; thus a relatively small error in the determination of the relative $l=0$ and 2 admixtures could produce a large error in the $l=2$ spectroscopic factor. The presence of $l=0$ components for transitions to the 1.37- and 9.83-MeV levels is tentative because the evidence for such a component is based entirely on the forwardmost data point. A DWBA prediction for a pure $l=2$ ($1d_{5/2}$) transition is shown (dotted line) for comparison with the angular distributions of these two levels. Even though several forward-angle data points are missing from the angular distribution of the 9.96-MeV level, it is grouped with the admixed $l=0+2$ transitions because of the known[11] spin and parity ($J^\pi=1^+$) of that state.

Angular distributions characteristic of $l=2$ and of $l=1$ transfers are contained in Figs. 4 and 5, respectively. In Fig. 4 the solid lines correspond to DWBA predictions based on $1d_{5/2}$ transfer, and the broken lines are for $1d_{3/2}$ transfer. Similarly, in Fig. 5 the solid and broken lines are for $2p_{3/2}$ and $1p_{1/2}$ transfer, respectively. The classifications of the transitions to the 10.82 and 10.16 states as $l=2$ and $l=1$, respectively (see Figs. 4 and 5), must be considered tentative. The agreement between the predicted and measured angular distributions is not as good for these two levels as for the other $l=1$ and 2 transitions. For both these states, the DWBA prediction for the alternate l value is also shown (as a dotted curve). The angular distribution of the weakly populated 6.00-MeV state is grouped with the $l=2$ transitions (Fig. 4) because that state is known[11] to have a spin and parity of 4^+.

The angular distribution of the 8.44-MeV doublet[11] [$J^\pi=(4^+)+1^-$] is shown in Fig. 5 together with curves obtained from an admixture of $l=1$ and 2 DWBA predictions. These curves were calculated assuming $1d_{5/2}$ transfer for the $l=2$ component and both $2p_{3/2}$ (solid curve) and $1p_{1/2}$ (broken curve) transfer for the $l=1$ component. The relative strengths of the $l=1$ and 2 transitions were calculated using a χ^2-minimization fit to the data.

The remaining angular distributions are displayed in Fig. 6 and correspond to weaker transitions that do not exhibit strippinglike structure.

Spectroscopic factors were extracted using Eq.

TABLE II. Matrix elements and sum rules for predicting spectroscopic factors for various configurations [see Eq. (3) and text].

Configuration	K_f, T	$\lvert\langle\chi_f\lvert a^\dagger\rvert\chi_i\rangle\rvert^2$	g^2	$\sum_{njlJ_f}\frac{2J_f+1}{2J_i+1}S_{nlj}$ [a]
$(\frac{3}{2}^+[211])^2$	0, 0	$W(\alpha,\nu)^2$	2	$2\sum_{njl} W(\alpha,\nu)^2$
b	c	$\frac{1}{2}W(\alpha,\nu)^2$	$1+\delta(K_f,0)$	$\sum_{njl} W(\alpha,\nu)^2$

[a] For deformed harmonic-oscillator wave functions $\sum_{nlj} W(\alpha,\nu)^2=1$. For normalization of wave functions using Woods-Saxon potential see text and Ref. 36.

[b] Configurations where extra core nucleons are not in the same Nilsson orbit.

[c] $K=\Omega_1+\Omega_2$ and $|\Omega_1-\Omega_2|$, $T=0$ and 1.

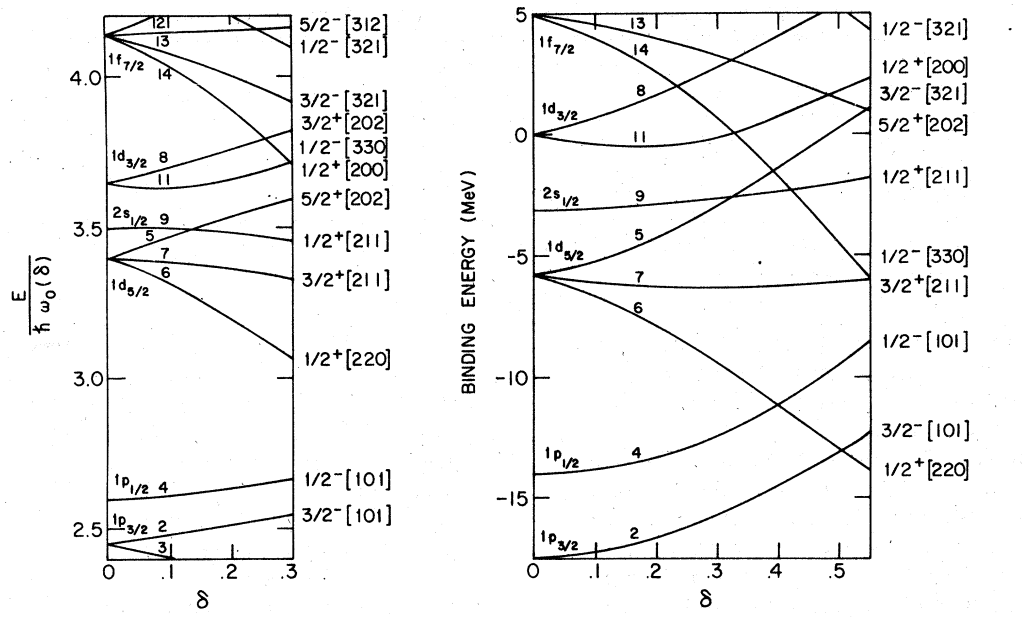

FIG. 7. Binding energies of proton states (right) as calculated in a deformed Woods-Saxon potential (Refs. 29, 31, 38). Also shown (left) for comparison are deformed harmonic-oscillator calculations (Ref. 39). The results are shown for positive deformation as a function of the Nilsson ellipsoidal deformation parameter δ.

(1) and are given in Table III for all states whose angular distributions were compared with DWBA predictions. The normalization constant N for the DWBA calculation was taken[40] to be 4.42. The isospin coupling coefficient C^2 is $\frac{1}{2}$ for ^{23}Na(^{3}He, d) transitions to both $T=0$ and $T=1$ final states in ^{24}Mg. If the $l=1$ DWBA cross sections had been calculated for $1p$ transfer rather than $2p$ transfer, the tabulated spectroscopic factors would have increased by a factor of 2.1 at $E_x=10.16$ MeV and 2.4 for $E_x=7.56$ MeV.

The magnitudes of the absolute spectroscopic factors depend directly on the absolute cross-section measurement and on the absolute magnitudes of the DWBA predictions. Since significant uncertainties exist in both of these quantities (e.g., a 30% uncertainty has already been placed on the absolute cross section, and the uncertainty in the DWBA analysis is probably of the same magnitude) a test of the absolute normalization for this particular study is desired. The in-band sum rule (Table II) provides such a test for the two known rotational bands[11] and for an additional band which is suggested in the present study (see Sec. V). Normalizing the spectroscopic factors to these in-band sum rules gives the empirically determined values of N that are listed in Table IV. Values of N were computed for both pure $d_{5/2}$ and pure $d_{3/2}$ transfer for the $l=2$ transitions to the $K=1$ and 2 bands of the $\frac{3}{2}^+[211]$, $\frac{1}{2}^+[211]$ configuration. The Nilsson-model spectroscopic factors are larger for $d_{3/2}$ transfer than for $d_{5/2}$ transfer for the states based on the $\frac{3}{2}^+[211]$, $\frac{1}{2}^+[211]$ configuration (see Table VI). However, it is known[36] that the experimentally determined spectroscopic factors for $j=l-\frac{1}{2}$ may be overestimated by the type of spin-orbit potential used in the DWBA calculations. Thus, the most accurate value of N is probably somewhere between the values listed in Table IV for $1d_{5/2}$ and $1d_{3/2}$ transfer. The agreement of the empirically determined values of N with the conventional value[40] ($N=4.42$) lends support to our absolute cross-section normalization and to the DWBA calculations. Unless otherwise stated, all spectroscopic factors discussed below were calculated assuming $N=4.42$.

An uncertainty of 35% is assigned to the measured absolute spectroscopic factor for states reached by a single l transfer. When the transition proceeds by two l values, a 50% uncertainty is assigned because of uncertainties inherent in the determination of relative admixtures of the two l values.

Information regarding the filling of the subshells may be obtained from the appropriate single-nucleon-transfer sum rules.[41] The summed ^{23}Na(^{3}He, d) spectroscopic strengths up to 11 MeV are compared in Table V with the predicted[41] s-d shell values assuming a ($1d_{5/2}$) (Ref. 7) configuration for the ^{23}Na ground state. Most of the $T=0$, $l=2$ strength, but only 28% of the $T=0$, $l=0$ strength, is observed below 11 MeV. The large

TABLE III. Results of the ^{23}Na(^{3}He, d)^{24}Mg reaction.

E_x [a] (MeV)	J^π lit [b]	l_p [c]	Assignment [c]	j_p	$(2J+1)S_l$ [d]	S_l [e]
1.37	2^+	(0) + 2		$\frac{5}{2}$	6.54	1.31
				$\frac{1}{2}$	0.16	0.03
				$\frac{3}{2}$	9.15	1.83
				$\frac{1}{2}$	0.19	0.04
4.12	4^+	2		$\frac{5}{2}$	0.53	0.06
4.23	2^+	0 + 2		$\frac{5}{2}$	2.32	0.46
				$\frac{1}{2}$	0.48	0.10
				$\frac{3}{2}$	3.40	0.68
				$\frac{1}{2}$	0.48	0.10
5.22	3^+	2		$\frac{5}{2}$	1.90	0.27
				$\frac{3}{2}$	2.61	0.37
6.00	4^+	(2)		$\frac{5}{2}$	$\lesssim$0.15	$\lesssim$0.02
6.44	0^+	f				
7.35	2^+	0 + 2		$\frac{5}{2}$	0.21	0.04
				$\frac{1}{2}$	0.18	0.04
				$\frac{3}{2}$	0.31	0.06
				$\frac{1}{2}$	0.18	0.04
7.56	1^-	1		$\frac{3}{2}$	0.03	0.01
				$\frac{1}{2}$	0.04	0.01
7.62	3^-	g				
7.75	1^+	0 + 2		$\frac{5}{2}$	1.15	0.38
				$\frac{1}{2}$	0.65	0.22
				$\frac{3}{2}$	1.60	0.53
				$\frac{1}{2}$	0.66	0.22
7.81	(5^+)	g				
8.12	(6^+)	g				
8.36	3^-	1		$\frac{3}{2}$	0.17	0.02
8.44	$(4^+) + 1^-$	1 + (2)		$\frac{5}{2}$	1.95	0.22
				$\frac{3}{2}$	0.56	0.19
				$\frac{5}{2}$	2.08	0.23
				$\frac{1}{2}$	0.57	0.19
8.65	2^+	0 + 2		$\frac{5}{2}$	0.83	0.17
				$\frac{1}{2}$	0.68	0.14
				$\frac{3}{2}$	1.16	0.23
				$\frac{1}{2}$	0.68	0.14
8.86	2^-	1		$\frac{3}{2}$	0.68	0.14
				$\frac{1}{2}$	0.78	0.16
9.00	2^+	g				
9.15	1^-	g				

TABLE III. *(Continued)*.

E_x [a] (MeV)	J^π lit [b]	l_p [c]	Assignment [c]	j_p	$(2J+1)S_l$ [d]	S_l [e]
9.28	$(2^+, 3^-, 4^+)$	2	$2^+, 4^+(0^+)$ [h]	$\frac{5}{2}$	1.16	
				$\frac{3}{2}$	1.62	
9.46	$(2^-, 3^+, 4^-)$	2	$3^+(1^+)$ [i]	$\frac{5}{2}$	0.98	0.14
				$\frac{3}{2}$	1.33	0.19
9.52	$4^+, T=1$ $+(6^+)$	2		$\frac{5}{2}$	2.39	0.26
9.83	(1^+)	$(0)+2$	$1^+(0^+, 2^+, 3^+, 4^+)$	$\frac{5}{2}$	1.07	0.36
				$\frac{1}{2}$	0.09	0.03
				$\frac{3}{2}$	1.46	0.49
				$\frac{1}{2}$	0.08	0.03
9.96	$1^+(T=1)$	$(0+2)$ [j]		$\frac{5}{2}$	0.62 [j]	0.21 [j]
				$\frac{1}{2}$	0.35 [j]	0.12 [j]
				$\frac{3}{2}$	0.85 [j]	0.28 [j]
				$\frac{1}{2}$	0.35 [j]	0.12 [j]
10.02		k				
10.06	$2^+(T=1)$	$(0)+2$		$\frac{5}{2}$	1.45	0.29
				$\frac{1}{2}$	0.44	0.09
				$\frac{3}{2}$	1.85	0.37
				$\frac{1}{2}$	0.46	0.09
10.16		(1)	$(0^-, 1^-, 2^-, 3^-)$	$\frac{3}{2}$	0.30	
				$\frac{1}{2}$	0.33	
10.35	2^+	2		$\frac{5}{2}$	2.24	0.45
				$\frac{3}{2}$	3.01	0.60
10.58		g				
10.66	0^+	g				
10.72	$1^+(T=1)$	$0+2$		$\frac{5}{2}$	0.95	0.32
				$\frac{1}{2}$	2.33	0.78
				$\frac{3}{2}$	1.31	0.44
				$\frac{1}{2}$	2.32	0.77
10.82		(2)	$[3^+(0^+, 1^+, 2^+, 4^+)T=1]^1$	$\frac{5}{2}$	0.25	0.04
				$\frac{3}{2}$	0.31	0.04
10.92	2^+	2		$\frac{5}{2}$	0.35	0.07
				$\frac{3}{2}$	0.49	0.10

[a] Excitation energies from Refs. 9 and 10.
[b] Spin and parity assignments from the literature as summarized in Refs. 4, 11, and 12.
[c] Parentheses indicate tentative assignment.
[d] Based on normally accepted $N=4.42$ (Ref. 40).
[e] Based on $N=4.42$ and spin assignment or preference in column 2 or 4. If no spin preference is given this column is left blank.
[f] Not excited.
[g] No stripping pattern observed. See Fig. 6 for angular distribution.
[h] Assignment based on known natural parity state and $2^+, 4^+$ preference from γ decay (Ref. 4).

TABLE III. *(Continued)*.

[i] Spin assignment based on known unnatural parity assignment and preference for 3^+ from γ decay (Ref. 4).

[j] Forward angle points covered by impurity (see Fig. 3); therefore spectroscopic factors may have very large errors.

[k] Covered by impurity.

[l] Preference for spin 3 based on comparison with ^{24}Na level scheme; see Secs. V E and V F of text.

fraction of the $l=0$ strength not accounted for below 11 MeV probably is a result of the large predicted $l=0$ spectroscopic factors (see Table VI) for transitions to the $\frac{1}{2}^+[200]$ Nilsson configuration if large deformations are assumed. The levels based on this configuration are predicted at high excitations (see Fig. 7). The Nilsson model also predicts[31,39] some $2s_{1/2}$ strength already filled in the ^{23}Na ground state. Indeed, $l=0$ strength is observed in pickup reactions on ^{23}Na, e.g. ~5% of the total possible $2s_{1/2}$ strength is observed as $l=0$ ^{23}Na(^{3}He, α) transitions[42] to states below an excitation of 7.5 MeV in ^{22}Na. In the present reaction, the $T=1$, $l=0$ spectroscopic strength below 11 MeV is larger than the $T=0$, $l=0$ strength (Table V). This can be understood if one assumes a smaller deformation for the $T=1$ states than for the $T=0$ states. For small deformations the $l=0$ strength is concentrated in the $\frac{1}{2}^+[211]$ Nilsson configuration. For larger deformations, however, it is predicted to shift largely to the $\frac{1}{2}^+[200]$ configuration (see Table VI and Refs. 29 and 31), which is predicted to be higher in excitation energy (see Fig. 7). Additional evidence suggesting a smaller deformation for the $T=1$ levels than for the $T=0$ states is presented in Sec. V F.

Nilsson-model spectroscopic factors, calculated using Eq. (3) and the Woods-Saxon wave functions,[31] are presented in Table VI, ignoring band mixing. The calculations assumed the ^{23}Na ground state consisted of one proton and two neutrons in the $\frac{3}{2}^+[211]$ Nilsson orbit with all lower orbits filled (Fig. 7). When two j's contribute for a particular l value, it is the sum of the calculated spectroscopic factors for the two j's that should be compared with the experimental spectroscopic factors.

V. DISCUSSION

A. States in the ground-state rotational band

The ground-state rotational band of ^{24}Mg is well established[1,3,4] (see Fig. 1). In terms of the collective model these states are described as a rotational band based on completely filled $\frac{1}{2}^+[220]$ and $\frac{3}{2}^+[211]$ Nilsson orbitals outside an ^{16}O core (see Fig. 7). The left-hand column of Fig. 8 compares the measured and predicted $l=2$ spectroscopic factors for the 2^+ and 4^+ members of the ground-state band. The solid horizontal lines correspond to the experimental spectroscopic factors with the hatched area representing the assigned errors. Whenever it is possible for the transfer to proceed by two j's, the experimental spectroscopic factor shown is the one extracted for the j value having the larger predicted spectroscopic factor (see Table VI). The theoretical spectroscopic factors for the two j's, of course, have been summed. The curves in Fig. 8 are the predicted spectroscopic factor as a function of the deformation. The ground state is not included, since a complete angular distribution was not measured for it. The predicted spectroscopic factors for the 2^+ and 4^+ members of this band are not strong functions of the deformation. The agreement between mea-

TABLE IV. ^{23}Na(^{3}He, d)^{24}Mg empirical normalization constants calculated using the inband sum rules of Table II.

Configuration	E_x	J^Π	K^Π	N $1d_{5/2}$ [a]	N $1d_{3/2}$ [a]
$(\frac{3}{2}^+[211])^2$	0.0	0^+ [b]	0^+	4.93	···
	1.37	2^+			
	4.12	4^+			
$\frac{3}{2}^+[211], \frac{1}{2}^+[211]$	4.23	2^+	2^+	3.61	2.65
	5.22	3^+			
	6.00	4^+			
$\frac{3}{2}^+[211], \frac{1}{2}^+[211]$	7.75	1^+	1^+	3.80 [c]	3.06 [c]
	8.65	2^+			
	(9.46)	3^+			
	c	4^+			
Theory [d]				$N=4.42$	

[a] Columns labeled $1d_{5/2}$ and $1d_{3/2}$ calculated from $l=2$ spectroscopic factors corresponding to transfer to corresponding subshell (Table III) for $J=1,2,3$. $J=0$ and 4 calculated for $1d_{3/2}$ and $1d_{5/2}$ spectroscopic factors, respectively.

[b] Spectroscopic factor $S(l=2)=0.05$ for ground state taken from Ref. 3.

[c] $J^\Pi=4^+$ member of band not known. Spectroscopic factor for 4^+ band member of band taken to be 0.04 (see Table VI).

[d] Reference 40.

TABLE V. Summed spectroscopic strengths.

	$\sum_{J_f}\frac{2J_f+1}{2J_i+1}C^2S_{lj}$ (predicted) [a]			Assumed	$\sum_{J_f}\frac{2J_f+1}{2J_i+1}C^2S_{lj}$(exp) [b]		
l	$T=0$	$T=1$	Total	j	$T=0$	$T=1$	Total
2	4	3	7	$\frac{5}{2}$	2.69 [c]	0.71	3.40 [c]
				$\frac{3}{2}$	3.62 [c]	0.84	4.46 [c]
1	...	...	...	$\frac{3}{2}$	0.22	d	0.22
				$\frac{1}{2}$	0.24	d	0.24
0	1	1	2	$\frac{1}{2}$	0.28	0.39	0.67

[a] Predicted (Ref. 41) assuming ^{23}Na ground state is of $(1d_{5/2})$ (Ref. 7) configuration.

[b] Based on a normalization constant of 4.42 (Ref. 40). Values are tabulated for DWBA calculations based on $1d_{5/2}$ and $1d_{3/2}$ transfer (see Table III) and $2p_{3/2}$ and $1p_{1/2}$ transfers. If only one j value is allowed by the selection rules the corresponding spectroscopic factor is included in either summation.

[c] Spectroscopic factor $S(l=2)=0.05$ for the ground state taken from Ref. 3.

[d] Lowest known negative-parity state in ^{24}Na is at 3.37 MeV (Ref. 45) which corresponds to about 12.9 MeV in ^{24}Mg.

sured and predicted spectroscopic factors is excellent for the 2^+ member of this band; however, the predicted spectroscopic factor for the 4^+ member is greater than that observed. In ^{22}Na, the 4^+ member of the $K=0$, $T=1$ band based on two particles in the same $\frac{3}{2}^+[211]$ Nilsson orbital also was observed to be populated more weakly than predicted in the ^{21}Ne(^{3}He,d)^{22}Na reaction.[31] The ^{23}Na(^{3}He,d) transitions to these states in ^{24}Mg are predicted to proceed by pure $l=2$ proton transfer, since the transferred proton enters an orbit having $\Omega^\pi=\frac{3}{2}^+$. A small $l=0$ component ($S_{\rm exp}=0.03$) is probably observed (Table III) in the transition to the 2^+ member of this band, and is thus an indication of a small amount of band mixing.

B. $T=0$ states based on the $3/2^+[211]$, $1/2^+[211]$ Nilsson configuration

An excited $K=2$ rotational band has been suggested[1,3-5] in ^{24}Mg. The configuration of this band has been described[3] in terms of the Nilsson model as consisting of unpaired nucleons in the $\frac{3}{2}^+[211]$ and $\frac{1}{2}^+[211]$ Nilsson orbitals. The calculation of proton binding energies in a deformed Woods-Saxon potential (Fig. 7) suggests that the $\frac{1}{2}^+[211]$ orbital should lie below a $\frac{5}{2}^+[202]$ orbital only for a deformation $\delta \gtrsim 0.3$. Such deformations are consistent with the observed[8] quadrupole moments of ^{24}Mg. The comparison of measured spectroscopic factors with the predictions of the Nilsson model for the members of this $K=2$ band are also shown in Fig. 8. The agreement for the 4.23 MeV 2^+ and 5.22 MeV 3^+ states is consistent with the suggested configuration and a large deformation. However, for large deformations, the 6.00-MeV 4^+ member is predicted to be more strongly populated than observed. The 4^+ member of the ground-state band, the 4.12-MeV level, also was observed to be more weakly excited than predicted (Fig. 8 and Sec. V A).

In addition to the $K^\pi=2^+$ rotational band just discussed, there should be a $K^\pi=1^+$ band based on the same $\frac{3}{2}^+[211]$, $\frac{1}{2}^+[211]$ Nilsson configuration. The 1^+ band head of this rotational band is predicted (Table VI) to have a sizable $l=0$ (^{3}He,d) spectroscopic factor. The Nilsson model for large deformations [i.e., for deformations greater than that for which the $\frac{5}{2}^+[202]$ and $\frac{1}{2}^+[211]$ Nilsson orbits cross (see Fig. 7)] predicts that the lowest 1^+ state in ^{24}Mg should be this $K=1$ band head. Indeed, the lowest known 1^+ level in ^{24}Mg, at 7.75 MeV, is observed (Table III) to have a sizable $l=0$ (^{3}He,d) spectroscopic factor. The observed $l=0$ and 2 spectroscopic factors for this level are compared with the predictions of the Nilsson model in the left-hand column of Fig. 9. The experimentally observed $l=0$ value is in agreement with the predictions for $0.25 \lesssim \delta \lesssim 0.5$ whereas the $l=2$ value is in agreement only for $\delta \gtrsim 0.45$. The 2^+ member of this band is also predicted to be populated by a mixed $l=0+2$ (^{3}He,d) transition. The only candidate for such a state below 10 MeV is the 8.65-MeV 2^+ level [the 2^+ state at 9.00 MeV is not strongly populated in the (^{3}He,d) reaction (see Table III)]. Similarly, a state at 9.46 MeV, having $J^\pi=3^+(1^+)$ (Table III), can be associated with the 3^+ member of this band. The experimental spectroscopic factors for these 2^+ and 3^+ states are compared with the predicted values in

TABLE VI. Spectroscopic factors predicted from the rotational model.

Configuration $\Omega^{\Pi}[Nn_z\Lambda]$	K [a]	J^{Π}	l	J	S_{th} [b] $\delta=0.0$	$\delta=0.2625$	$\delta=0.525$
$(\frac{3}{2}^+[211])^2$	0	0^+	2	$\frac{3}{2}$	0.00	0.23	0.45
		2^+	2	$\frac{5}{2}$	1.37	1.30	1.21
				$\frac{3}{2}$	0.00	0.05	0.09
		4^+	2	$\frac{5}{2}$	0.13	0.12	0.11
$\frac{3}{2}^+[211],\frac{1}{2}^+[211]$	1	1^+	2	$\frac{5}{2}$	0.00	0.02	0.02
				$\frac{3}{2}$	0.00	0.13	0.23
			0	$\frac{1}{2}$	1.00	0.44	0.07
		2^+	2	$\frac{5}{2}$	0.00	0.06	0.09
				$\frac{3}{2}$	0.00	0.13	0.23
			0	$\frac{1}{2}$	0.20	0.09	0.01
		3^+	2	$\frac{5}{2}$	0.00	0.06	0.09
				$\frac{3}{2}$	0.00	0.04	0.07
		4^+	2	$\frac{5}{2}$	0.00	0.02	0.03
$\frac{3}{2}^+[211],\frac{1}{2}^+[211]$	2	2^+	2	$\frac{5}{2}$	0.00	0.03	0.04
				$\frac{3}{2}$	0.00	0.13	0.23
			0	$\frac{1}{2}$	0.80	0.35	0.05
		3^+	2	$\frac{5}{2}$	0.00	0.07	0.10
				$\frac{3}{2}$	0.00	0.09	0.16
		4^+	2	$\frac{5}{2}$	0.00	0.04	0.05
$\frac{3}{2}^+[211],\frac{5}{2}^+[202]$	1	1^+	2	$\frac{5}{2}$	0.67	0.67	0.67
		2^+	2	$\frac{5}{2}$	0.29	0.29	0.29
		3^+	2	$\frac{5}{2}$	0.07	0.07	0.07
		4^+	2	$\frac{5}{2}$	0.01	0.01	0.01
$\frac{3}{2}^+[211],\frac{5}{2}^+[202]$	4	4^+	2	$\frac{5}{2}$	0.44	0.44	0.44
$\frac{3}{2}^+[211],\frac{1}{2}^+[200]$	1	1^+	2	$\frac{5}{2}$	0.00	0.00	<0.01
				$\frac{3}{2}$	0.40	0.25	0.06
			0	$\frac{1}{2}$	0.00	0.36	0.55
		2^+	2	$\frac{5}{2}$	0.00	<0.01	0.02
				$\frac{3}{2}$	0.40	0.25	0.06
			0	$\frac{1}{2}$	0.00	0.07	0.11
		3^+	2	$\frac{5}{2}$	0.00	<0.01	0.02
				$\frac{3}{2}$	0.11	0.07	0.02
		4^+	2	$\frac{5}{2}$	0.00	0.00	0.01
$\frac{3}{2}^+[211],\frac{1}{2}^+[200]$	2	2^+	2	$\frac{5}{2}$	0.00	0.00	0.01
				$\frac{3}{2}$	0.40	0.25	0.06
			0	$\frac{1}{2}$	0.00	0.29	0.44
		3^+	2	$\frac{5}{2}$	0.00	0.00	0.02
				$\frac{3}{2}$	0.29	0.18	0.05
		4^+	2	$\frac{5}{2}$	0.00	0.00	0.01

TABLE VI. *(Continued)*.

Configuration $\Omega^{\Pi}[Nn_z\Lambda]$	K [a]	J^{Π}	l	J	S_{th} [b] $\delta=0.0$	$\delta=0.2625$	$\delta=0.525$
$\frac{3}{2}^+[211],\frac{1}{2}^-[330]$	1	1^-	3	$\frac{5}{2}$	0.00	<0.01	≤0.01
			1	$\frac{3}{2}$	0.00	0.18	0.15
				$\frac{1}{2}$	0.00	0.05	0.09
		2^-	3	$\frac{7}{2}$	0.06	0.03	0.02
				$\frac{5}{2}$	0.00	≤0.01	≤0.06
			1	$\frac{3}{2}$	0.00	0.16	0.13
				$\frac{1}{2}$	0.00	0.02	0.03
		3^-	3	$\frac{7}{2}$	0.19	0.09	0.07
				$\frac{5}{2}$	0.00	≤0.01	≤0.06
			1	$\frac{3}{2}$	0.00	0.05	0.04
		4^-	3	$\frac{7}{2}$	0.19	0.09	0.07
				$\frac{5}{2}$	0.00	<0.01	≤0.02
		5^-	3	$\frac{7}{2}$	0.06	0.03	0.02
$\frac{3}{2}^+[211],\frac{1}{2}^-[330]$	2	2^-	3	$\frac{7}{2}$	0.01	0.01	0.01
				$\frac{5}{2}$	0.00	≤0.01	≤0.02
			1	$\frac{3}{2}$	0.00	0.16	0.13
				$\frac{1}{2}$	0.00	0.04	0.07
		3^-	3	$\frac{7}{2}$	0.12	0.06	0.04
				$\frac{5}{2}$	0.00	≤0.02	≤0.06
			1	$\frac{3}{2}$	0.00	0.12	0.10
		4^-	3	$\frac{7}{2}$	0.21	0.10	0.08
				$\frac{5}{2}$	0.00	≤0.01	≤0.03
		5^-	3	$\frac{7}{2}$	0.11	0.05	0.04

[a] $T=0$ for the $(\frac{3}{2}^+[211])^2$ configuration. Both $T=0$ and 1 components are allowed for the other configurations.

[b] Calculated using Eq. (3) and the Woods-Saxon wave functions of Ref. 31. Where it is possible for two j's to contribute for an l the sum of the calculated spectroscopic factors for the two j's should be compared with the experimental spectroscopic factors.

the center column of Fig. 9. Whereas the $l=2$ spectroscopic factors are consistent with the large deformations necessary to explain the transitions to the other states of this and the $(\frac{3}{2}^+[211])^2$ configurations, the observed $l=0$ spectroscopic factor for the 8.65-MeV 2^+ state is somewhat large.

C. $T=0$ states based on the $3/2^+[211], 5/2^+[202]$ Nilsson configuration

If the lowest excited, single-particle rotational bands in ^{24}Mg can be explained in terms of the $\frac{3}{2}^+[211]$, $\frac{1}{2}^+[211]$ Nilsson configuration, states based on the $\frac{3}{2}^+[211]$, $\frac{5}{2}^+[202]$ configuration should occur at only slightly higher excitation energies (Fig. 7). Based on the assumed configuration of the ^{23}Na ground state (paired $\frac{3}{2}^+[211]$ neutrons and an unpaired $\frac{3}{2}^+[211]$ proton outside a closed ^{20}Ne core), states based on the $\frac{3}{2}^+[211]$, $\frac{5}{2}^+[202]$ Nilsson configuration should be populated by pure $l=2$ (^{3}He,d) transitions (Table VI). Bands having $K^{\pi}=1^+$ and 4^+ arise from this configuration. In the absence of mixing between major shells, the predicted spectroscopic factors for these two bands are independent of the deformation. The 1^+ and 4^+ band heads and the 2^+ member of the $K^{\pi}=1^+$ band are predicted to be populated by strong $l=2$ (^{3}He,d) transitions (Table VI). The strongest predominantly $l=2$ transitions to possible 1^+, 2^+, and 4^+, $T=0$ states below 11 MeV are for the 9.83 MeV

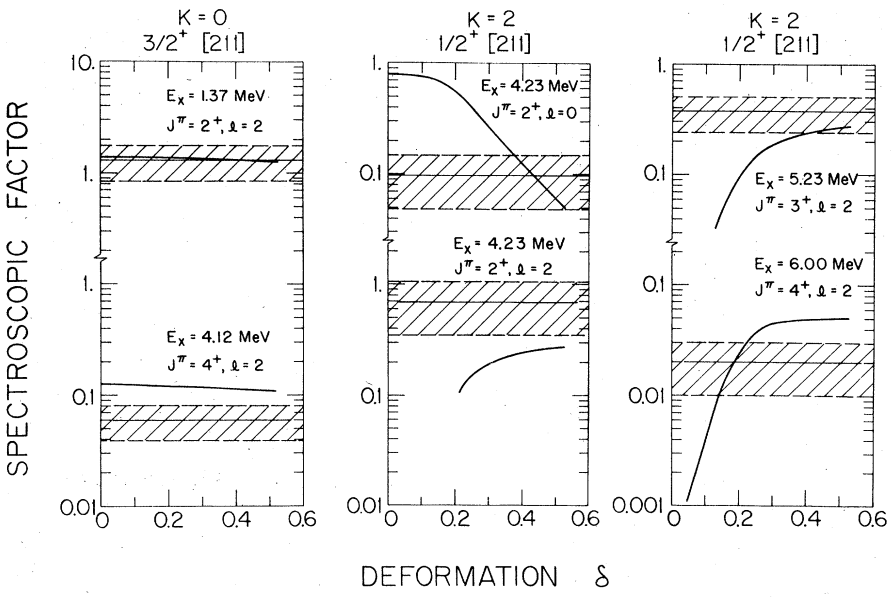

FIG. 8. Comparison of predicted and measured spectroscopic factors for members of the ground-state band (left) and the $K^\pi = 2^+$ band based on the $\frac{3}{2}^+$ [211], $\frac{1}{2}^+$ [211] Nilsson configuration (center and right). The solid horizontal lines are the experimental values, and the hatched area represents the assigned errors. When it is possible for the transfer to proceed by two j's, the experimental value shown corresponds to the j having the larger predicted spectroscopic factor. The curves are predictions of the rotational model (see text and Table VI) as a function of deformation. See Secs. V A and V B of the text for discussion.

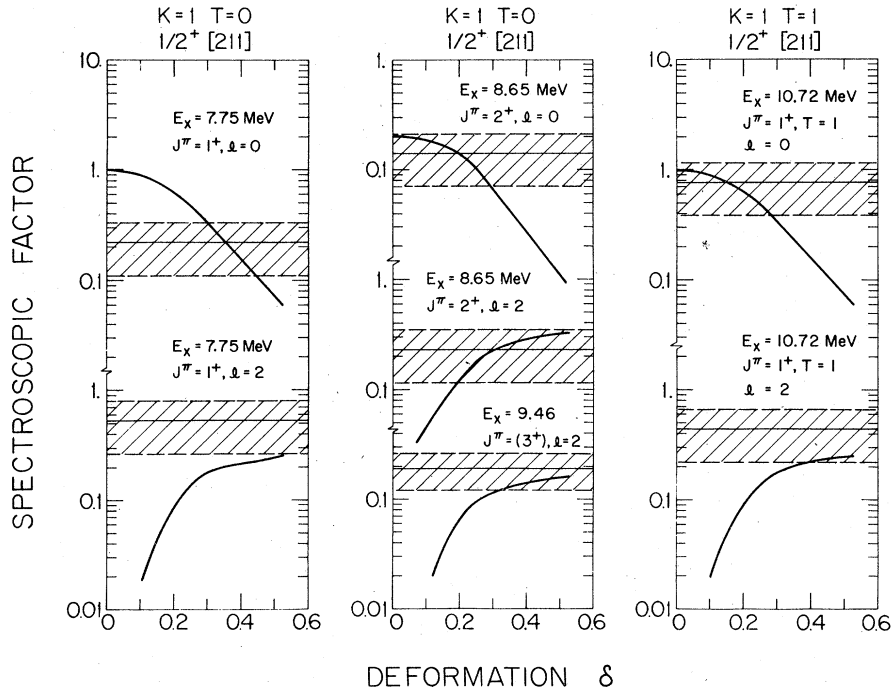

FIG. 9. Comparison of predicted and measured spectroscopic factors for members of the $T = 0$ (left and center) and $T = 1$ (right) $K^\pi = 1^+$ bands based on the $\frac{3}{2}^+$ [211], $\frac{1}{2}^+$ [211] Nilsson configurations. The description is the same as Fig. 8. See Secs. V B and V F of the text for discussion.

TABLE VII. Comparison of measured and predicted spectroscopic factors for states suggested to be based on the $\frac{3}{2}^+[211], \frac{5}{2}^+[202]$ configuration.

			$T=0$		$T=1$	
K	J^π	S_{th} [a]	E_x (MeV)	S_{exp} [b]	E_x (MeV)	S_{exp} [b]
1	1	0.66	9.83	0.36 ± 0.12	9.96	(0.21 ± 0.11) [c]
	2	0.29	10.35	0.45 ± 0.15	10.06	0.29 ± 0.10
	3	0.07			10.82	(0.036 ± 0.012)
	4	0.01				
4	4	0.44	8.44	0.23 ± 0.12	9.52	0.27 ± 0.09

[a] Calculated using Eq. (3) and Woods-Saxon wave functions (Ref. 31).
[b] From Table III for transfer to $1d_{5/2}$ subshell.
[c] The spectroscopic factor for this state is probably in error as the forward angles were covered by an impurity group. The separation of $l=0$ and 2 components without the forward angle data probably grossly underestimated the $l=2$ component. A spectroscopic factor of 0.47 ± 0.15 was observed for this transition in a recent ^{23}Na(d,n) reaction (Ref. 17).

$1^+(0^+, 2^+, 3^+, 4^+)$ state, the 10.35 MeV 2^+ state, and the 8.44 MeV (4^+) state, respectively (Table III). The $l=2$ experimental spectroscopic factors for these transitions are compared with the predicted values in Table VII. (The experimental values for the $T=1$ states of this same configuration also are given and will be discussed in Sec. V F.) The experimental spectroscopic factors for these transitions are observed to be somewhat less than the predicted values, with the transitions to the 1^+ and 4^+ band heads being only about 50% of the predicted values. In a ^{21}Ne(^{3}He, d)^{22}Na study[31] the most probable candidate for the 1^+ band head (at 3.94 MeV) based on this same configuration (unpaired $\frac{3}{2}^+[211]$ and $\frac{5}{2}^+[202]$ nucleons was also populated with only 50% of the strength predicted from the Nilsson model.

D. States based on negative-parity configurations

One of the successes of the Nilsson description in this mass region is its ability to account for observed low-lying negative-parity states.[31,32,42] For large positive deformations, two Nilsson configurations may account for low-lying, negative-parity states (Fig. 7): an unpaired particle in the $\frac{1}{2}^-[330]$ orbit or a hole in the $\frac{1}{2}^-[101]$ orbit. For deformations of $\delta > 0.45$ the levels based on a particle in the $\frac{1}{2}^-[330]$ Nilsson orbital would be predicted to be lower in excitation than those based on the $\frac{1}{2}^-[101]$ hole states. Such particle states in ^{24}Mg would be expected to be populated appreciably in the ^{23}Na(^{3}He, d) reaction (Table VI). The low-lying negative-parity states at 7.56, 7.62, and 8.36 MeV were only weakly populated in this study (Table III). A 2^- state at 8.86 MeV is, however, populated with appreciable strength in the ^{23}Na(^{3}He, d) reaction. The known[4] 1^- state at 8.44 MeV also seems to have an appreciable $l=1$ transition strength (Table III). The extracted $l=1$ transition strength for this level has a greater uncertainty than for the other levels, since it was necessary to separate it from the $l=2$ (^{3}He, d) transition to the nearby probable[4] 4^+ state. (The similarity of the angular distributions of the $l=1$ and 2 transitions at this Q value increases the difficulty of obtaining an accurate separation of these transition strengths.) The experimental spectroscopic factors for these two states are compared with Nilsson-model predictions in Fig. 10. The (^{3}He, d) spectroscopic factors of the 8.44-MeV 1^- state and the 8.86-MeV 2^- state are in good agreement (for large deformations) with the predictions corresponding to the

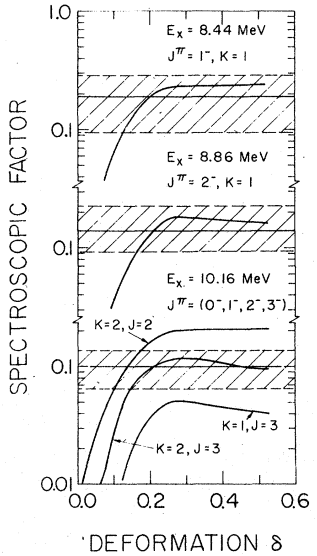

FIG. 10. Comparison of predicted and measured spectroscopic factors for states based on the $\frac{3}{2}^+$ [211], $\frac{1}{2}^-$ [330] Nilsson configuration. The description is the same as Fig. 8. See Sec. V D of the text for discussion.

TABLE VIII. Comparison of present work with earlier ^{23}Na(^{3}He, d) and ^{23}Na(d, n) results.

E_x (MeV)	Present work [a] l	Present work [a] $(2J_f+1)C^2S$	^{23}Na(^{3}He, d) [b] l	^{23}Na(^{3}He, d) [b] $(2J_f+1)C^2S$	^{23}Na(d, n) [c] l	^{23}Na(d, n) [c] $(2J_f+1)C^2S$
0.0	d	d	2	0.025	2	0.14 ± 0.06
1.37	(0) + 2	(0.08) + 3.27	2	5.5	2	3.08 ± 0.60
4.12	2	0.26	2	0.45	2	≤0.60
4.23	0 + 2	0.24 + 1.16	0 + 2	0.65 + 1.50	0 + 2	0.34 + 0.70 ± 0.20
5.22	2	0.95	2	1.68	2	1.12 ± 0.32
6.00	2	≲0.08	2	0.27	2	≤0.14
7.35	0 + 2	0.09 + 0.10			0 + 2	0.08 + (0.30)
7.56	1	0.02				
7.75	0 + 2	0.32 + 0.58			{0 + 2	0.40 + 0.90 ± 0.32
7.81	e					
8.36	1	0.08				
8.44	1 + (2)	0.28 + (1.04)			1 + 2	0.42 ± 0.12 + 2.2 ± 0.6
8.65	0 + 2	0.34 + 0.41			0 + 2	0.40 + 0.90 ± 0.20
8.86	1	0.39			1	0.72 ± 0.06
9.00	e		0 + (2)	0.04	+ (0.40)	
9.15	e				1 + 3	0.12 ± 0.02 + 1.6 ± 0.4
9.28	2	0.58				
9.46	2	0.49			{2	2.14 ± 0.40
9.52	2	1.20				
9.83	(0) + 2	(0.04) + 0.54				
9.96	(0 + 2) [f]	(0.18 + 0.31) [f]			2	0.70 ± 0.22
10.06	(0) + 2	(0.22) + 0.72			0 + 2	0.28 + 1.00 ± 0.40
10.16	(1)	0.16				
10.35	2	1.12			2	0.48 ± 0.16
10.74	0 + 2	1.16 + 0.48			0 + 2	1.24 + 0.8 ± 0.4
10.82	(2)	0.12				
10.92	2	0.18				

[a] Except when selection rules select $d_{3/2}$ and $p_{3/2}$ tabulated values of the spectroscopic factors correspond to transfer to $1d_{5/2}$ subshell for $l=2$ and to $1p_{1/2}$ for $l=1$ (Table III). For transfer to $1d_{3/2}$ subshell the spectroscopic factor would be from 30 to 60% larger (see Table III).

[b] From Ref. 3 for a bombarding energy of 35 MeV.

[c] From Ref. 17 for a bombarding energy of 6 MeV.

[d] Not measured.

[e] Not strongly populated (see Table III and Figs. 2 and 6).

[f] Missing data at forward angles; therefore separation of $l=0$ and 2 may be grossly in error.

1^- and 2^- members of a $K^\pi = 1^-$ rotational band based on unpaired nucleons in the $\frac{3}{2}^+[211]$ and $\frac{1}{2}^-[330]$ Nilsson orbitals. A probable $l=1$ transition to the 10.16-MeV state (see Fig. 5), however, is stronger than that predicted for the 3^- member of the $K^\pi = 1^-$ band of this configuration, and is weaker than that predicted (assuming large deformations) for the bandhead of a $K^\pi = 2^-$ band based on this configuration. A measurement of the spin of this level is necessary to determine its configuration. Moderately strong $l=1$ transitions have been observed[17] in the ^{23}Na(d, n) reaction to states at 11.31 and 11.39 MeV in ^{24}Mg. These states, therefore, may be the members of the $K^\pi = 2^-$ rotational band based on the $\frac{3}{2}^+[211]$, $\frac{1}{2}^-[330]$ Nilsson configuration.

The 3^- state at 7.62 MeV, which was only weakly populated in the ^{23}Na(^{3}He, d) reaction, was observed to be moderately populated in a ^{25}Mg(^{3}He, α) study,[43] suggesting that this state may be a hole state based on the $\frac{5}{2}^+[202]$, $\frac{1}{2}^-[101]$ configuration. (The $\frac{5}{2}^+$ ground state of ^{25}Mg is described in the simple rotational model as an unpaired $\frac{5}{2}^+[202]$ neutron outside a ^{24}Mg core.) States of such a configuration would be expected to be populated strongly in a pickup reaction.

E. Comparison with other single-proton stripping reactions leading to ^{24}Mg

The results of the present study are compared with those of an earlier ^{23}Na(^{3}He, d) study[3] (at an incident energy of 35 MeV) and with a ^{23}Na(d, n) study[17] (at an incident energy of 6 MeV) in Table VIII. Results of a more recent ^{23}Na(d, n) study,[12] performed with 5.5-MeV incident deuterons, were

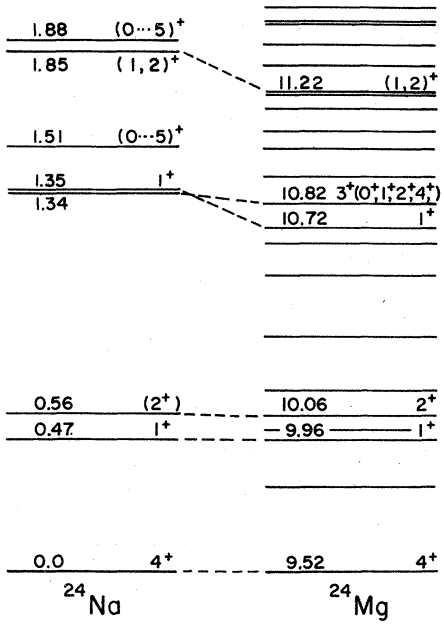

FIG. 11. Comparison of the excitation energies of the low-lying levels in ^{24}Na with those for the $T=1$ levels of ^{24}Mg. All known levels in ^{24}Mg between 9.5 and 11.5 MeV in excitation are shown, and excitation energies are listed for the suggested $T=1$ states. Isobaric analogs are connected by broken lines. See Sec. V F of the text for a discussion of the $T=1$ states.

not included since the values of the spectroscopic factors from that work were consistently a factor of 3–4 below the corresponding values from the other works. The values of the spectroscopic strengths from the earlier ^{23}Na(^{3}He,d) study[3] are consistently larger than those of the present study. For most levels the spectroscopic strengths from the ^{23}Na(d,n) study[17] agree with the present values to within the assigned errors; however, the $l=0$ spectroscopic factors from the (d,n) study, which have smaller assigned errors, are about 20% larger than those for the corresponding levels in the present work.

F. $T=1$ states

The spectrum of known $T=1$ states in ^{24}Mg is compared in Fig. 11 with the low-lying levels of ^{24}Na (Refs. 11, 44, and 45). The 4^+ ground state[11] of these $T=1$ nuclei can be explained in terms of the Nilsson model as consisting of unpaired nucleons in the $\frac{3}{2}^+[211]$ and $\frac{5}{2}^+[202]$ Nilsson orbitals. In ^{24}Mg, however, $T=0$ states based on the $\frac{3}{2}^+[211]$, $\frac{1}{2}^+[211]$ configuration (e.g. the 4.23-MeV 2^+ state) are observed considerably lower in excitation than states based on the $\frac{3}{2}^+[211]$, $\frac{5}{2}^+[202]$ configuration—the lowest probably being the 8.44-MeV (4^+) state (see Sec. V C). In terms of the pure Nilsson model, this implies that the $T=0$ states of mass 24 have a larger deformation than the $T=1$ states (Fig. 7). The lowest three known $T=1$ levels in ^{24}Mg (the 9.52-MeV 4^+, the 9.96-MeV 1^+, and the 10.06-MeV 2^+ states) may be explained as the lowest members of $K^\pi=4^+$ and 1^+ bands based on unpaired nucleons in the $\frac{3}{2}^+[211]$ and the $\frac{5}{2}^+[202]$ orbitals. The transfer of a proton to the $\frac{5}{2}^+[202]$ orbital requires a pure $l=2$ transition and its transition strength is independent of deformation (Table VI). The experimentally observed $l=2$ spectroscopic factors for these states are compared with the predicted values in Table VII. The experimental values are observed to be about 50% of the predicted values. The experimental single-nucleon-transfer spectroscopic factors for the $T=0$ states that are suggested to be of this configuration in ^{24}Mg (see Sec. V C and Table VII) and in ^{22}Na (see Ref. 31) also were smaller than predicted in the simple Nilsson model. The sizable $l=0$ strength observed in the (^{3}He,d) transition to the 9.96-MeV level (Table III) may be in error, since the forward three data points were covered in an impurity group (see Fig. 2). (Larger angle data are relatively insensitive to $l=0$ components in the transition.) This level was observed[17] to be populated by a pure $l=2$ ^{23}Na(d,n) transition. If the $l=0$ (^{3}He,d) strength of this transition is zero the $l=2$ component would increase to ~0.9; however, the predicted angular distribution then differs considerably from the observed distribution. The ^{23}Na(d,n) $l=2$ spectroscopic factor[17] for the transition to the 9.96-MeV state is 0.47 ± 0.15. This value, while being less than the predicted value, is consistent with the transition to the $T=0$ state of the same configuration (Table VII). A small $l=0$ component is possibly observed for the transition to the 2^+ state at 10.06 MeV ($S_{exp}=0.09$). The observed $l=0$ components in the transitions to the 9.96- and 10.06-MeV leads are indicative of configuration mixing. The experimental spectroscopic factor (assuming $T=1$) for the probable 3^+ state at 10.82 MeV is compared (in Table VII) with the predicted value for the 3^+ $T=1$ member of the $K^\pi=1^+$ band based on the $\frac{3}{2}^+[211]$, $\frac{5}{2}^+[202]$ configuration. Additional evidence supporting the identification of this level as the analog of the 1.34-MeV level of ^{24}Na (Fig. 11) comes from the comparison of the results of this study with a ^{23}Na(d,p)^{24}Na study[44] discussed below. Similar to the transitions to the other states based on this configuration in this study and in the ^{21}Ne(^{3}He,d) study,[31] the strength of this transition also is observed to be only about 50% of that predicted.

A second 1^+ $T=1$ state is known at 10.72 MeV in ^{24}Mg. Since this level is populated in the (^{3}He,d) reaction with a large $l=0$ component (Fig. 3 and

TABLE IX. Comparison of the ^{23}Na$(d,p)^{24}$Na and ^{23}Na$(^3$He$,d)^{24}$Mg spectroscopic factors.

^{23}Na$(d,p)^{24}$Na [a]				^{23}Na$(^3$He$,d)^{24}$Mg [b]							
E_x (MeV)	J^π	$(2J_f+1)S(0)$	$(2J_f+1)S(2)$	E_x (MeV)	J^π	$(2J_f+1)S(0)$	$(2J_f+1)S(2)$	ΔE_c (keV)	Assumed [c] J^π	K^π [c]	Assumed [c] configuration
0.00	4^+	···	2.76	9.517	4^+	···	2.39	4784 ± 6	4^+	4^+	$\frac{3}{2}^+[211], \frac{5}{2}^+[202]$
0.4723	1^+	(0.056)	1.56	9.984	1^+	(0.35) [d] [–] [e]	(0.62) [d] [7.40] [e]	4779 ± 16	1^+	1^+	$\frac{3}{2}^+[211], \frac{5}{2}^+[202]$
0.5633	(2^+)	0.40	(1.20)	10.072	2^+	(0.44)	1.45	4776 ± 8	2^+	1^+	$\frac{3}{2}^+[211], \frac{5}{2}^+[202]$
				10.822	$3^+(0^+,1^+,2^+,4^+)$	···	(0.25)	4748 ± 20	3^+	1^+	$\frac{3}{2}^+[211], \frac{5}{2}^+[202]$
1.341	1^+	2.48	(1.48)	10.737	1^+	2.32	1.31	4658 ± 9	1^+	1^+	$\frac{3}{2}^+[211], \frac{1}{2}^+[211]$
1.511	$(0\cdots5)^+$	···	···	f					5^+	4^+	$\frac{3}{2}^+[211], \frac{5}{2}^+[202]$
1.846	$(1,2)^+$	0.80	(1.56)	11.223	$(1,2)^+$	[0.88]	[1.60] [c]	4644 ± 10	2^+	1^+	$\frac{3}{2}^+[211], \frac{1}{2}^+[211]$
1.885	$(0\cdots5)^+$	···	1.16	f					4^+	1^+	$\frac{3}{2}^+[211], \frac{5}{2}^+[202]$

[a] Excitation energies from Ref. 11, spectroscopic strengths from Ref. 44, and spin assignments from Ref. 45.
[b] Excitation energies from Ref. 11 and spectroscopic strengths and spin assignments from Table III.
[c] Assumed spin, parity, K, and configurations from Ref. 45. See also text (Sec. V F).
[d] Large errors expected in these spectroscopic factors as forward angle data are covered by an impurity group.
[e] Values in brackets are from a ^{23}Na$(d,n)^{24}$Mg study (Ref. 17).
[f] Corresponding isobaric analog in ^{24}Mg not known.

Table III), it is suggested as the $K^\pi = 1^+$, $T = 1$ band head based on the $\frac{3}{2}^+[211]$, $\frac{1}{2}^+[211]$ configuration. The experimental spectroscopic factors observed for the (^{3}He, d) transition to this level are compared with the predictions of the Nilsson model in the right-hand column of Fig. 9. The $l = 0$ spectroscopic factor is in agreement with the predicted values for deformations of $\delta \lesssim 0.30$, whereas the $l = 2$ spectroscopic factor agrees only for a deformation of $\delta \gtrsim 0.35$. The observation of the $T = 1$ levels based on the $\frac{3}{2}^+[211]$, $\frac{5}{2}^+[202]$ configuration lower in excitation than the levels from the $\frac{3}{2}^+[211]$, $\frac{1}{2}^+[211]$ implies a deformation of $\delta \lesssim 0.30$. It is known (e.g. see Sec. IV) that a small change in the $l = 0$ spectroscopic factor will produce a much larger difference in the $l = 2$ spectroscopic factor. Thus, the spectroscopic factors observed for the 10.72-MeV level are probably consistent with the suggestion that the $T = 1$ states of mass 24 are less deformed than the $T = 0$ states.

Table IX compares the spectroscopic factors observed[44] in the ^{23}Na(d,p)^{24}Na reaction at 7.8-MeV incident energy with the ^{23}Na(^{3}He, d) spectroscopic factors for the $T = 1$ levels at ^{24}Mg from the present study. Energy shifts of the corresponding isobaric analogs and suggested configurations are also tabulated. The agreement of the spectroscopic factors for the analogs is within the expected DWBA uncertainties. Except for the identification of the 1.34-MeV level of ^{24}Na with the 10.82-MeV level of ^{24}Mg, the correspondence of the analogs has previously been suggested.[11] The 10.82-MeV level of ^{24}Mg [which is populated by a probable $l = 2$ ^{23}Na(^{3}He, d) transition] is suggested as the analog of the probable 3^+ state[44] at 1.341 MeV in ^{24}Na. This identification is based on the fact that the energy shift for this level is nearly the same as those for the other analog pairs, and that the (^{3}He, d) spectroscopic factor for this transition is consistent with those for transitions to other members of the $\frac{3}{2}^+[211]$, $\frac{5}{2}^+[202]$ configurations (Table VIII). The 10.82-MeV level is not populated by either the ^{20}Ne(^{7}Li, d)^{24}Mg or the ^{20}Ne(^{6}Li, d)^{24}Mg reactions,[26] which should only populate $T = 0$ final states. The Coulomb shift corresponding, respectively, to the 1.347- and 1.846-MeV level of ^{24}Na and the 10.74- and 11.22-MeV level of ^{24}Mg is less than for the other analog pairs, and is consistent with these states being of a different configuration from the other $T = 1$ levels compared in Table IX.

Analogs of the 1.51- and 1.88-MeV states of ^{24}Na are not known in ^{24}Mg (see Fig. 11). The results of a ^{25}Mg(d, ^{3}He)^{24}Na study[45] suggest the 1.51-MeV level as the 5^+ member of the ^{24}Na ground-state rotational band ($K^\pi = 4^+$ based on the $\frac{3}{2}^+[211]$, $\frac{5}{2}^+[202]$ two-particle Nilsson configuration). Therefore, this level would not be populated by the single-nucleon stripping reaction on a ^{23}Na target. Indeed the 1.51-MeV level is not observed in the ^{23}Na(d,p)^{24}Na study.[44] The ^{25}Mg(d, ^{3}He)^{24}Na study[45] also suggests that the 1.88-MeV level is the 4^+ member of the $K^\pi = 1^+$ band of the $\frac{3}{2}^+[211]$, $\frac{5}{2}^+[202]$ configuration. Such a state is predicted in the Nilsson model to be weakly populated [$S(l = 2) = 0.01$] in the single-nucleon stripping reaction on a ^{23}Na target (see Table VII). This level in ^{24}Na was possibly more strongly populated in the ^{23}Na(d,p) reaction[44] (see Table IX).

VI. CONCLUSIONS

The experimentally measured spectroscopic factors for the $T = 0$ states based on the $(\frac{3}{2}^+[211])^2$ and the $\frac{3}{2}^+[211]$, $\frac{1}{2}^+[211]$ configurations are in general agreement (i.e., within the uncertainties of the DWBA calculations) with the predictions of the Nilsson model for deformations of $\delta \approx 0.4$–0.5, with the exception of the 4.12 and 6.00 4^+ states. If the harmonic-oscillator wave functions of Chi[39] had been used instead of the Woods-Saxon wave functions, the experimental spectroscopic factors would have been consistent with a somewhat smaller deformation. The experimental $l = 0$ spectroscopic factors for the $K^\pi = 1^+$, $T = 0$ band based on the $\frac{3}{2}^+[211]$, $\frac{1}{2}^+[211]$ configuration, however, are larger than the predictions for large deformations (Fig. 9). (This discrepancy seems to suggest a smaller deformation.) An equally likely explanation could be that the $l = 0$ (^{3}He, d) transition strengths for these states are enhanced due to mixing. In fact, some mixing is probably observed in the transition to the 2^+ member of the ground-state band. [An apparent small $l = 0$ component is observed in the transition to this state (Fig. 3), whereas the (^{3}He, d) transition to this state is predicted to be pure $l = 2$ (Table VI).] The transitions to the 4^+ states at 4.12 and 6.00 MeV are considerably weaker than predicted. In a ^{21}Ne(^{3}He, d)^{22}Na study[31] the 4^+ member of the $K^\pi = 0^+$ band based on the $(\frac{3}{2}^+[211])^2$ configuration was also more weakly populated than predicted.

Several states have been suggested as the $T = 0$ and 1 members of the $\frac{3}{2}^+[211]$, $\frac{5}{2}^+[202]$ configuration. In these cases the measured spectroscopic factors, which are predicted to be independent of the deformation (Table VII), are only about $\frac{1}{2}$ of the predicted values. Similarly, the observed experimental ^{21}Ne(^{3}He, d) spectroscopic factor for a state in ^{22}Na suggested to be based on this same configuration was only half that predicted.[31] This observed reduction of transition strength for the states based on the $\frac{3}{2}^+[211]$, $\frac{5}{2}^+[202]$ configuration may be qualitatively understood in terms of con-

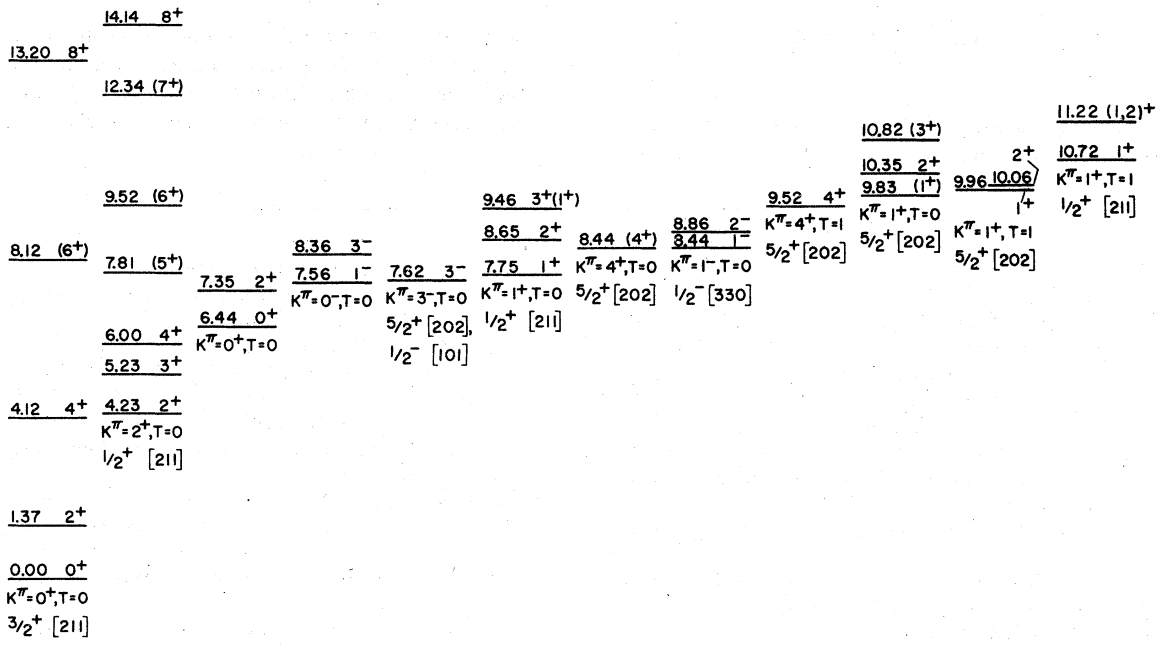

FIG. 12. Summary of rotational bands in ^{24}Mg. The $K^\pi = 0^+$ and 0^- bands with band head at 6.44 and 7.56 MeV respectively are probably based on multiparticle-multihole configurations, and the $K^\pi = 3^-$ band with a bandhead at 7.62 MeV is assumed to be based on unpaired nucleons in the $\frac{5}{2}^+$ [202] and $\frac{1}{2}^-$ [101] Nilsson levels. The assumed configuration of the remaining bands is a nucleon in the $\frac{3}{2}^+$ [211] Nilsson orbit coupled to a nucleon in the orbit listed for each band.

figuration mixing. For example, if the ground state of ^{23}Na contained a large component of the $\frac{3}{2}^+$ part of the $\frac{1}{2}^+$[211] configuration, spectroscopic factors for transitions to final states of the $\frac{3}{2}^+$[211], $\frac{5}{2}^+$[202] configuration would be expected to be reduced relative to those of the $\frac{3}{2}^+$[211], $\frac{1}{2}^+$[211] configuration. Such an explanation, however, would also imply a reduction in the transitions to other configurations e.g. the negative-parity states, which seem to be in satisfactory agreement with the predictions. Pure $l=2$ (^{3}He, d) transitions are predicted for states based on the $\frac{3}{2}^+$[211], $\frac{5}{2}^+$[202] configurations (Table VII). Small $l=0$ transitions, however, are observed for the 1^+ and 2^+ states based on this configuration—again indicating mixing.

The known negative-parity states at 8.44 and 8.86 and a possible negative-parity state at 10.16 MeV are moderately populated in the present study, indicating that such states may be formed by adding a proton to the $\frac{1}{2}^-$[330] Nilsson orbit. The 3^- state at 7.62 MeV, which was not populated strongly in the present study, is moderately populated by the ^{25}Mg(^{3}He, α) reaction,[43] indicating that this level may be of the $\frac{5}{2}^+$[202], $\frac{1}{2}^-$[101] configuration.

The known and suggested rotational bands of ^{24}Mg are summarized in Fig. 12. Whenever an identification of an experimental state with a given Nilsson configuration is considered tentative, its excitation energy is listed in parentheses. The Nilsson configuration and K quantum number for each band that is suggested to be based on single-particle excitations are given below the band head.

Nilsson model configurations have been suggested for all the states of ^{24}Mg below 9.0 MeV except for the 6.44-MeV 0^+ state, the 7.35-MeV 2^+ state, the 7.56-MeV 1^- state, and the 8.36-MeV 3^- state. These states, which were only weakly excited in the present study (Table III), are strongly excited in the α-particle transfer reactions.[26-28] The 6.44-MeV 0^+ and 7.35-MeV 2^+ states have previously been suggested[19] as the 0^+ and 2^+ members of a $K^\pi = 0^+$ rotational band based on a multiparticle-multihole configuration. Similarly, the remaining 7.56-MeV 1^- and 8.36-MeV 3^- states may be the lowest two members of a $K^\pi = 0^-$ band. Such a band, observed starting at 5.80 MeV in ^{20}Ne, is strongly populated by the ^{16}O(^{7}Li, t) reaction.[46] These two bands are also indicated in Fig. 12.

In summary, configurations have been suggested for most of the levels of ^{24}Mg below 11 MeV. However, most of the predicted (^{3}He, d) transition strength for states based on the $\frac{3}{2}^+$[211], $\frac{5}{2}^+$[202] configuration is missing. Also, it is necessary to assume that the $T=1$ states are less deformed than the $T=0$ states in order to explain the properties of the lowest $T=1$ states.

ACKNOWLEDGMENTS

The authors wish to thank P. Neogy for his assistance in performing the experiment, P. Nicolaides for her careful scanning of the nuclear emulsions, and B. Pomerantz and J. Cizewski for their assistance in the data analyses. We acknowledge financial support from the National Science Foundation.

---

*Present address: Niels Bohr Institute, 17 Blegdamsvej, Copenhagen, Denmark.
†Currently at KVI, Groningen, on leave from University of Pennsylvania.
‡Present address: Department of Physics, State University of New York 12203.

[1]See e.g., G. Rakavy, Nucl. Phys. 4, 375 (1957).
[2]S. Nilsson, K. Dan. Vidensk. Selsk. Mat.-Fys. Medd. 29, No. 16 (1955) and B. R. Mottelson and S. Nilsson, *ibid*. 1, No. 8 (1959).
[3]R. C. Bearse and J. L. Yntema, Phys. Rev. 175, 1442 (1968).
[4]R. Ollerhead, J. Kuehner, R. Levesque, and E. Blackmore, Can. J. Phys. 46, 1381 (1968).
[5]A. Cohen and J. Cookson, Nucl. Phys. 29, 604 (1962).
[6]D. Branford, N. Gardner, and I. F. Wright in *Proceedings of the International Conference on Properties of Nuclear States, Canada*, 1969, edited by M. Harvey *et al*. (Presses de l'Université de Montréal, Montréal, Canada, 1969), p. 112.
[7]Y. Akiyama, A. Arima, and T. Sebe, Nucl. Phys. A138, 273 (1969).
[8]D. Schwalm and B. Povh, Phys. Lett. 29B, 103 (1969); see also A. Bamberger, P. G. Bizzeti, and B. Povh, Phys. Rev. Lett. 21, 1599 (1968); O. Häusser, B. W. Hooton, D. Pelte, T. K. Alexander, and H. C. Evans, *ibid*. 22, 359 (1969) and Can. J. Phys. 48, 35 (1970).
[9]S. Hinds and R. Middleton, Proc. Phys. Soc. (London) 76, 553 (1960).
[10]S. Hinds, R. Middleton, and A. Litherland, Proc. Phys. Soc. (London) 77, 1210 (1961).
[11]P. Endt and C. van der Leun, Nucl. Phys. A105, 1 (1967).
[12]S. N. Tang, B. D. Sowerby, and D. M. Sheppard, Nucl. Phys. A125, 289 (1969).
[13]P. W. M. Glaudemans and P. M. Endt, Nucl. Phys. 42, 367 (1963).
[14]N. P. Baumann, F. W. Prosser, Jr., W. G. Read, and R. W. Krone, Phys. Rev. 104, 376 (1956).
[15]E. Goldberg, W. Haeberli, A. I. Galonsky, and R. A. Douglas, Phys. Rev. 93, 799 (1954).
[16]P. J. M. Smulders, Physica 31, 973 (1965); G. J. Highland and T. T. Thwaites, Nucl. Phys. A109, 163 (1968); R. H. Spear and I. F. Wright, Aust. J. Phys. 21, 307 (1968).
[17]H. Fuchs, K. Grabisch, P. Kraaz, and G. Roschert, Nucl. Phys. A122, 59 (1968).
[18]E. F. Bennett, Phys. Rev. 122, 595 (1961).
[19]R. C. Haight, Ph.D. thesis, Princeton University, 1969 (unpublished).
[20]E. W. Hamburger and A. G. Blair, Phys. Rev. 119, 777 (1960).
[21]D. Dehnhard and C. Mayer-Böricke, Nucl. Phys. A97, 164 (1967).
[22]See e.g., M. E. Rickey, H. E. Wegner, and K. W. Jones, Phys. Rev. Lett. 13, 444 (1964).
[23]R. Middleton, J. D. Garrett, and H. T. Fortune, Phys. Rev. Lett. 24, 1436 (1970).
[24]D. P. Balamuth, J. E. Holden, J. W. Noé, and R. W. Zurmühle, Phys. Rev. Lett. 26, 1271 (1971).
[25]A. Gobbi, P. R. Maurenzig, L. Chua, R. Hadsell, P. D. Parker, M. W. Sachs, D. Shapira, R. Stockstad, R. Wieland, and D. A. Bromley, Phys. Rev. Lett. 26, 396 (1971).
[26]R. Middleton, in *Proceedings of the International Conference on Nuclear Reactions Induced by Heavy Ions, Heidelberg, Germany*, 1969, edited by R. Bock and W. R. Hering (North-Holland, Amsterdam, The Netherlands, 1970), p. 263.
[27]P. Neogy, W. Scholz, J. Garrett, and R. Middleton, Phys. Rev. C 2, 2149 (1970).
[28]J. D. Garrett and R. Middleton, Bull. Am. Phys. Soc. 14, 549 (1969); J. D. Garrett, in the Proceedings of the Symposium on Two-Nucleon Transfer and Pairing Excitations, ANL report, 1972.
[29]J. D. Garrett, R. Middleton, D. J. Pullen, S. A. Andersen, O. Nathan, and O. Hansen, Nucl. Phys. A164, 449 (1971).
[30]P. D. Kunz, University of Colorado Report No. COO-535-613 (unpublished).
[31]J. D. Garrett, R. Middleton, and H. T. Fortune, Phys. Rev. C 4, 165 (1971).
[32]J. R. Powers, H. T. Fortune, R. Middleton, and O. Hansen, Phys. Rev. C 4, 2030 (1971).
[33]H. T. Fortune, N. G. Puttaswamy, and J. L. Yntema, Phys. Rev. 185, 1546 (1969).
[34]J. L. Yntema and G. R. Satchler, Phys. Rev. 134, B976 (1964).
[35]H. T. Fortune, T. J. Gray, W. Trost, and N. R. Fletcher, Phys. Rev. 179, 1033 (1969).
[36]J. D. Garrett, R. Middleton, and H. T. Fortune, Phys. Rev. C 2, 1243 (1970).
[37]G. R. Satchler, Ann. Phys. (N.Y.) 3, 275 (1958).
[38]S. Wahlborn and G. Ehrling (private communication); see Refs. 29 and 31.
[39]B. Chi, Nucl. Phys. 83, 97 (1966).
[40]R. H. Bassel, Phys. Rev. 149, 791 (1966).
[41]See, e.g. J. P. Schiffer, in *Isospin in Nuclear Physics*, edited by D. H. Wilkinson (North-Holland, Amsterdam, The Netherlands, 1969), p. 665.
[42]J. D. Garrett, H. T. Fortune, and R. Middleton, Phys. Rev. C 4, 1138 (1971).
[43]M. Shalaby, M. El-Bedewi, J. D. Garrett, R. Middleton, and H. T. Fortune (to be published).
[44]C. Daum, Nucl. Phys. 45, 273 (1963).
[45]E. Kramer, G. Mairle, and G. Kaschl, Nucl. Phys. A165, 353 (1971).
[46]R. Middleton, B. Rosner, D. J. Pullen, and L. Polsky, Phys. Rev. Lett. 20, 118 (1968).